

# MERITS OF PULSE MODE OPERATION OF RESIDUAL GAS IONIZATION PROFILE MONITOR FOR J-PARC MAIN RING\*

Kenichirou Satou<sup>†</sup>, Susumu Igarashi, and Yoichi Sato, J-PARC/KEK, Tokai, Japan

## Abstract

The measurement accuracy of the ionization profile monitor (IPM) of J-PARC main ring (MR) depends on the flatness and stability of the gain of the position-sensitive microchannel plate (MCP). The flatness of the MCP deteriorates after long-term operation; the gain of the central area selectively decreases as the integrated output charge increases. The beam-based calibration, where the local bump shifts the beam and the reconstructing beam profiles determine the gain distribution, is used to calibrate the flatness. The immediate gain drop occurs when the output current from the MCP becomes comparable to the bias current is problematic. This gain drop depends on the bias voltage and the output current; thus, it is difficult to calibrate. A pulsed HV module of 30 kV, which collects ionized electrons and ions, was installed to solve these problems. The pulse mode operation can modulate the averaged output current from the MCP to improve gain stability. Profiles of the intense beam up to  $3.3E13$  particles per bunch were measured and compared with those measured by destructive profile monitors in beam transport lines 3–50 BT, and the Abort line. Estimated emittances were consistent at  $\pm 20\%$ .

## INTRODUCTION

The idea of detecting ionized electrons or ions generated by the interaction with residual gas to measure a beam profile was reported in the mid-1960s [1, 2]. The residual gas ionization profile monitor (IPM) has been widely used in proton and hadron synchrotrons because of its non-invasiveness to the beam since it does not insert solid material or gas into the beam. A small rate of nuclear collision with residual gas particles is preferable to a high-power proton synchrotron on its low beam power loss and thus lower induced remnant dose.

The first IPM system in KEK was used at KEK-PS [3], where the system collected positive ions using an external electric field ( $E_{ex}$ ). These ions were detected using a microchannel plate (MCP). Similar monitors were designed for the J-PARC main ring (MR) and installed in 2008 [4-6]. These were operated in the ion collection using an intensive  $E_{ex}$  of 50 kV across 130 mm-size cage electrodes at the maximum. A horizontal type IPM (D2HIPM) and a vertical type IPM (D2VIPM) were installed in a straight line named *Ins\_B*, where the horizontal dispersion function is zero. However, another horizontal type IPM (D3HIPM) is installed in the arc section, named *Arc\_C*, where the horizontal dispersion function was non-zero. The Twiss parameters at these IPMs are  $(\beta_x, \beta_y, \eta_x) = (12.1 \text{ m}, 27.3 \text{ m}, 0 \text{ m})$ ,

(13.1 m, 21.6 m, 0 m), and (8.4 m, 15.5 m, 2.0 m) for D2VIPM, D2HIPM, and D3HIPM, respectively. The MCPs are a two-stage type with 32 multi-strip anodes of 2.5 mm (in width), a glass tube with 15  $\mu\text{m}$  in diameter, and an effective area of 30 mm  $\times$  80 mm. The resistances are 112 M $\Omega$  for D2HIPM and 120 M $\Omega$  for D2HIPM, respectively.

A fast data-taking system has realized the turn-by-turn (TxT) measurement. The TxT profiles are used widely in correction of dipole and quadrupole injection mismatches [7]. However, it was strenuous to measure beam emittance due to the strong beam space charge ( $E_{sc}$ ) of MV/m level, signal purity contaminated with secondary electrons, and MCP's dynamic gain deterioration that occurred several msec after the electron multiplication occurred.

We modified the original DC type IPM to a gated IPM, where the pulsed  $E_{ex}$  is applied to switch the system in  $\sim 20 \mu\text{s}$  to solve the MCP's dynamic gain deterioration. The remaining sections describe this IPM system for J-PARC MR and the merits of pulse mode operation. Finally, the estimated accuracy of the system checked with the multi-ribbon profile monitors (MRPMs) in beam transport lines is presented.

## IPM IMPROVEMENTS

At the initial stage of beam commissioning, where the beam intensity is 1/10 of the designed intensity of 4E13 ppb, three IPM systems were designed to collect positive ions with strong  $E_{ex}$  [4-6].

The dipole magnets were installed only in the D2HIPM to collect electrons against strong  $E_{sc}$  to measure an intense beam of several E13 particles per bunch (ppb) [8]. The guiding dipole field of  $B_g = 0.2 \text{ T}$  was applied parallel to the vertical component  $E_{ext}$ , which was used to direct the electrons to the MCP. The  $B_g$  and the horizontal  $E_{sc}$  ( $E_{sc-x}$ ) component produce an  $E \times B$  drift motion, which converts the transversal kick by the  $E_{sc-x}$  to the longitudinal drift motion.

Measuring only the ionized electrons, which are  $\sim 1000$  electrons per bunch, is challenging. The contaminant of secondary electrons degenerates the signal purity and the measurement accuracy. To subdue the secondary electrons generated by the ion's impacts on the electrodes, we applied a simple idea of using a window on cage electrodes to collect the ions and demonstrated it first on IPM for the CERN PS [9]. This structure is called an ion trap. Applying the same idea subdues the secondaries onto the MCP detector and improves signal purity significantly [10].

It is necessary to check the difference in signal intensity between the ion and electron collection to check the signal purity; besides the detection efficiency of MCP, which is 10%–60% for electrons and 60%–85% for ions, in the case

\* Work supported by Accelerator and Beamline Research and Technology Development for High-Power Neutrino Beams in the U.S.-Japan Science and Technology Cooperation Program in High Energy Physics.

<sup>†</sup> email address: kenichirou.satou@j-parc.jp

of the total kinetic energy of 2 ~ 50 keV, the signal intensities should be the same.

Finally, we used the pulse mode operation idea to improve our system. The pulse mode operation is realized at the Fermi National Accelerator Laboratory (FNAL) [11]. The system used the pulsed HV to accelerate the ionized particles onto the MCP detector. By using this system, we can modify operating duty by changing the gate width and operational frequency. A gated system was designed and installed in the D2HIPM [10]. The IPM operated with the system is called a gated IPM.

### MERITS OF PULSE MODE OPERATION

By changing the gate width and timing, the gated IPM can modulate the duty of operation and monitor the signals at any time, for example, only 20 turn profiles after beam injection. The gated IPM has three merits.

The first is the extension of the MCP lifetime. Figure 1 shows an example of the measurement of gain flatness of the MCP, scanned with beams shifted horizontally by the local bump orbit. The initial gain of the MCP worsened as the integrated output charge increased in long-term usage. As shown in the Fig. 1 the gain at the center has decreased by approximately 40% since 2008. The lifetime of the MCP becomes much longer when the duty of the operation changes lower than 1%.

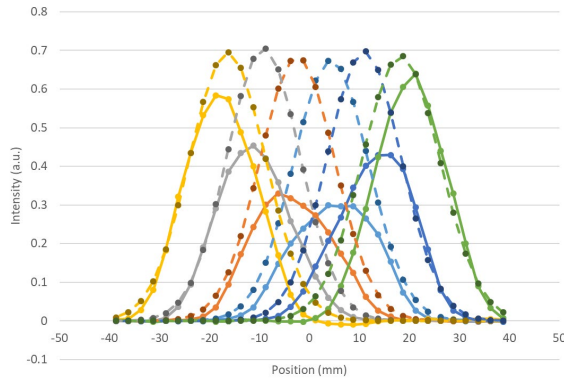


Figure 1: Gain balance measurement of MCP using a scanned beam shifted horizontally. Dashed lines are reconstructed profiles.

The second is to gain stability. Figure 2 shows the gain of a single-MCP glass tube (channel) modeled in [12] using a multi-dynodes model connected in parallel with the capacitor and resistor. Before the electron multiplication occurs, the capacitor is well charged. When a drain of a large current from a channel occurs, the stored charge in a capacitor decreases, and consequently, the local bias voltage. Thus, the local gain of the later stage of the dynodes decreases.

The output current limit should be 7% of the bias current of its channel (current channel) to maintain a flat gain. It also connects the channels in the in-plane direction. Fig. 3 shows that the sum of the signal from the MCP decreased immediately to 1/3 in 3 msec after the multiplication started. To measure profiles at, for example, 1 sec after the beam injection, fine-tuning of the bias voltage must ensure

that the local output current from the beam center is less than 7% of the channel current.

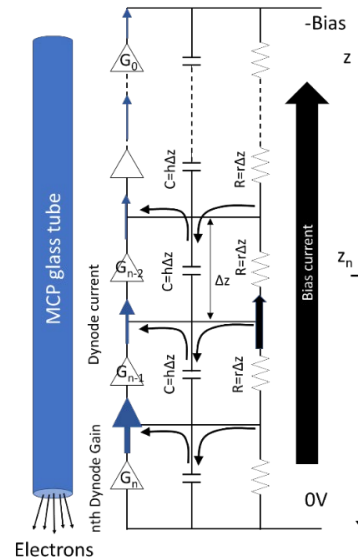


Figure 2: Multi-dynodes model of a single-MCP glass tube (channel).

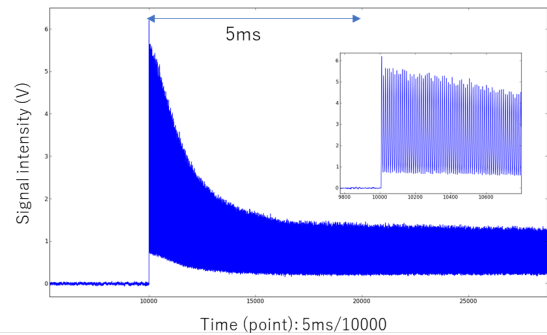


Figure 3: Total output current from the MCP, where the vertical scale factor is 1 V:10  $\mu$ A. The output current is comparable to the bias current of MCP, 18  $\mu$ A.

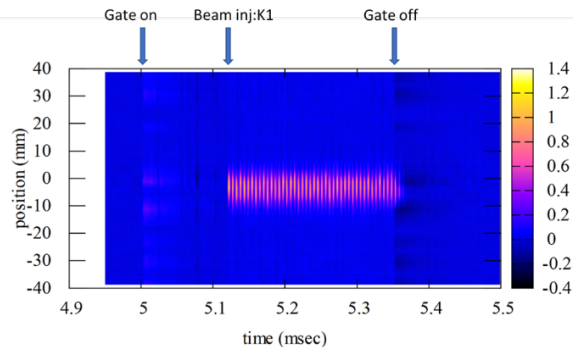


Figure 4: Signals from Gated IPM, just after the beam injection. The beam intensity was 2.4E13 ppb.

Under stable gain conditions, the gated IPM can select and measure beam profiles at any time. Figure 4 shows the cantor map and the sum signal of MCP, where the gate timing is selected for 20 turns after injection. The bias voltages were the same in both cases (Figs. 3 and 4).

The final is the stable gas pressure in the IPM chamber. The gated IPM, operated at 1% duty, did not change the gas pressure of  $2.5E-7$  Pa; the original IPM changed the gas pressure from  $2E-7$  Pa to  $7E-7$  Pa in about 10 sec. Stable gas pressure is preferable for checking the number of electrons detected from the output current.

## DISCUSSION: PERFORMANCE CHECK WITH DESTRUCTIVE PROFILE MONITORS

We used the gated IPM to measure profiles for the beam whose intensity was between  $2.4E12$  ppb and  $3.3E13$  ppb (83% of the designed intensity), where only 3 GeV 1 bunch beams from the RCS were injected and accelerated to 30 GeV. The MRPM was used to measure the beam at the beam transport line from RCS to MR (3–50 BT) and at the Abort line to dump the beams. Furthermore, we extracted the beams at 3 GeV and 30 GeV to the Abort line. Figure 5 shows the locations of the IPMs and MRPMs.

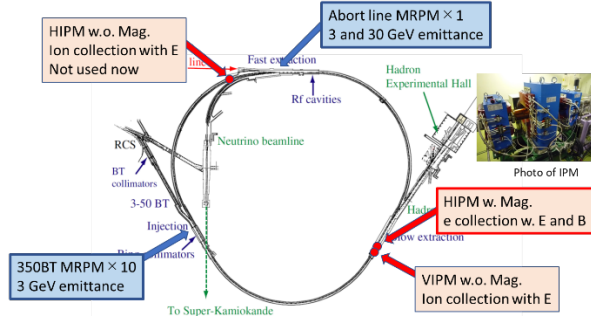


Figure 5: IPMs in MR and MRPMs in 3–50 BT and Abort line.

The HV and the  $B_g$  were set to  $-20$  kV and  $0.2$  T, respectively. Similarly, the MCP's bias voltage was at  $2.0$  kV. Furthermore, we set the gate width and timing to measure only 20-turn profiles after the injection and before extraction. During the measurements, the gas pressure in the chamber was stable at  $2.4E-7$  Pa. Also, we repeated the measurement 20 times, and the signals were recorded and averaged to reduce the statistical error due to the small number of ionized electrons estimated to be  $1.7E3$  ppb for the 30 GeV beams with an intensity of  $3.3E13$  ppb.

The root mean square (RMS) emittance from the gated IPM was estimated as,

$$\varepsilon = (\sigma_m^2 - \sigma_{anode}^2 - \sigma_{COD}^2) / \beta_x \quad (1)$$

where  $\sigma_m$  is the RMS width of a measured beam profile,  $\sigma_{anode}$  is the RMS width of the strip anode of the MCP, and  $\sigma_{COD}$  is the RMS of the deviation of the closed orbit distortion due to the ripple of the driving current to the bending magnets. The beam position monitors measured  $0.7$  mm  $\sigma_{COD}$  [13]. Also, the ripple currents to the quadrupole magnet modulate the  $\beta_x$ . However, the estimated error was

$\pm 0.3\%$  [13], which is negligible. The power supplies to the magnets are proposed to be replaced in 2022 [14] and the ripple will be improved to 1/10. Fig. 6 shows the profile measured at 3 GeV and 30 GeV, whose size is  $\sigma_m = 9.45$  and  $3.14$  mm, respectively.

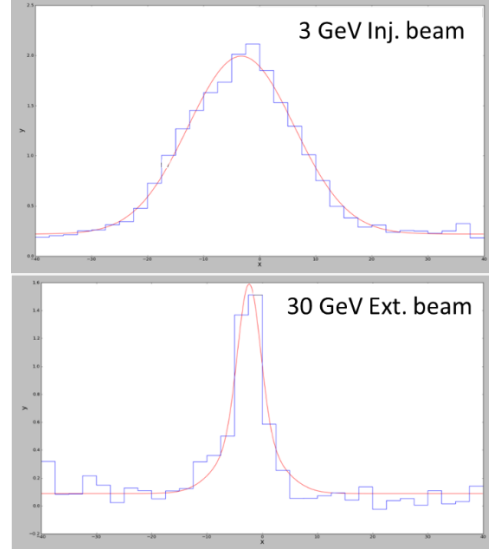


Figure 6: Profile measured by the gated IPM for the  $3.3E13$  ppb beam at injection and extraction energy. The blue lines are the measured profiles, and the red lines are the fitted results.

Figure 7 shows the beam parameters measured using the 10 MRPMs in 3–50 BT [15]. The beam intensity was  $1.25E13$  ppb. The solid lines represent the calculations using the optics parameters set to the 3–50 BT beam line. These calculations agree well with the measured data within an error of 4% in beam size.

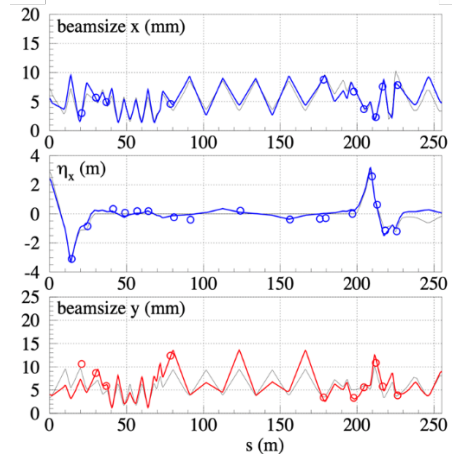


Figure 7: Beam parameters measured by the 10 MRPMs in 3–50 BT. Beam sizes for horizontal and vertical and dispersion function are shown with the calculation.

The beams whose intensity is  $3.3E13$  ppb, both the 3 GeV and 30 GeV cases, were also measured at the MRPM [16] in the Abort line. The Twiss parameters at the MRPM are  $(\beta_x, \beta_y, \eta_x) = (161 \text{ m}, 15.2 \text{ m}, -1.81 \text{ m})$  for 3 GeV and  $(147 \text{ m}, 34.8 \text{ m}, -1.78 \text{ m})$  for 30 GeV. The emittance was estimated as

$$\varepsilon = \frac{1}{\beta_x} \left\{ \sigma_m^2 - \sigma_{\text{ribbon}}^2 - \eta_x^2 \left( \frac{\Delta p}{p} \right)^2 \right\}, \quad (2)$$

where  $\sigma_{\text{ribbon}}$  is the RMS size of the ribbon and  $\Delta p/p$  denotes the momentum spread. The momentum spread is assumed to be 0.1% for both beams.

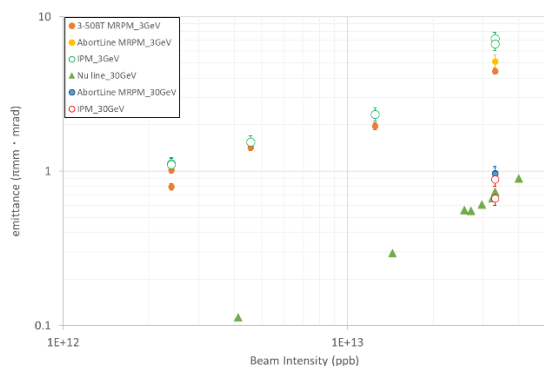


Figure 8: Emittance measured at the gated IPM and MRPMs. The open circles are from the gated IPM and the solid circles are from MRPMs. The solid triangle data were measured at the Neutrino beamline.

Figure 8 shows the estimated emittances. Also, we checked the estimated emittances using the data measured at the neutrino beamline [17, 18] at 30 GeV. The three datasets are consistent with each other by  $\pm 20\%$ . The data from the gated IPM are 15% higher than that of the 3–50 BT MRPM measurement. A part of this would have originated from the optics mismatch of 3–50 BT to the MR because optics of the 3–50 BT were deliberately detuned to reduce beam loss after an injection.

## SUMMARY

In this study, we improved the IPM system for J-PARC MR to measure electrons against strong  $E_{\text{sp}}$  and to eliminate secondary electrons. Furthermore, we upgraded it to a gated IPM system. Also, we have presented and elaborated on the three merits of the gated IPM. The beam emittance of intense beams up to  $3.3\text{E}13$  ppb was measured and compared with those from other profile monitors in the beam transport lines, 3–50 BT, Abort, and neutrino beamlines. The datasets used are consistent with each other by  $\pm 20\%$ .

## ACKNOWLEDGMENT

The author thanks Mr. J. R. Zagel and Dr. R. Thurman-Keup of the FNAL for their friendly and immense support received on the HV gate generator development and for several informative discussions on the gated IPM system.

## REFERENCES

[1] V. Dudnikov, “The intense proton beam accumulation in storage ring by charge-exchange injection method”, Ph.D. Thesis, INP, Novosibirsk, 1966; G. Budker, G. Dimov, and V. Dudnikov, in *Proc. Int. Symposium on Electron and Positron Storage Rings*, Saclay, France, 1966, Article No. VIII-6-1.

[2] F. Hornstra and W. H. Deluca, “Non-destructive beam profile detection systems for the ZGA”, ANL internal report, 1967.

[3] T. Kawakubo, T. Ishida, E. Kadokura, Y. Ajima, and T. Adachi, “Fast Data Acquisition System of a Non-Destructive Profile Monitor for a Synchrotron Beam by Using Micro Channel Plate with Multi-Anodes”, *Nucl. Instrum. Methods Phys. Res., Sect. A*, vol. 302, pp. 397-405, 1991. doi: 10.1016/0168-9002(91)90352-Q

[4] K. Satou *et al.*, “Beam Diagnostic System of the Main Ring Synchrotron of J-PARC”, in *Proc. HB'08*, Nashville, TN, USA, Aug. 2008, paper WGF11, pp. 472-474.

[5] K. Satou *et al.*, “Development of IPM for J-PARC MR”, in *Proc. 6<sup>th</sup> Accelerator Meeting in Japan*, Tokai, Aug. 2009, pp. 292-294.

[6] K. Satou, H. Harada, N. Hayashi, S. Lee, T. Toyama, and A. Ueno, “IPM Systems for J-PARC RCS and MR”, in *Proc. HB'10*, Morschach, Switzerland, Sep.-Oct. 2010, paper WEO1C05, pp. 506-510.

[7] G. H. Wei *et al.*, “Beam Tuning of Injection and Fast Extraction of J-PARC MR”, in *Proc. 6<sup>th</sup> Accelerator Meeting in Japan*, Tokai, Aug. 2009, pp. 307-309.

[8] K. Satou, H. Kuboki, and T. Toyama, “Profile Measurement by the Ionization Profile Monitor with 0.2T Magnet System in J-PARC MR”, in *Proc. IBIC'16*, Barcelona, Spain, Sep. 2016, pp. 811-814. doi: 10.18429/JACoW-IBIC2016-WEP669

[9] K. Satou, J. W. Story, S. Levasseur, G. Schneider, D. Bodart, and M. Sapinski, “A Novel Field Cage Design for the CPS IPM and Systematic Errors in Beam Size and Emittance”, *J. Phys. Conf. Ser.*, vol. 1067, 2018, p. 072008. doi: 10.1088/1742-6596/1067/7/072008

[10] K. Satou, “Development of Gated IPM System for J-PARC MR”, in *Proc. IBIC'19*, Malmö, Sweden, Sep. 8-12, 2019, pp. 343-346. doi: 10.18429/JACoW-IBIC2019-TUPP020

[11] J. R. Zagel *et al.*, “Third Generation Residual Gas Ionization Profile Monitors at Fermilab”, in *Proc. IBIC'14*, Monterey, CA, USA, Sep. 2014, paper TUPD04, pp. 408-411.

[12] L. Giudicotti, “Time-Dependent Model of Gain Saturation in Microchannel Plates and Channel Electron Multipliers”, *Nucl. Instrum. Methods Phys. Res., Sect. A*, vol. 659, pp. 336-347, 2011. doi: 10.1016/j.nima.2011.07.017

[13] T. Asami, private communication

[14] S. Igarashi *et al.*, “Accelerator Design for 1.3 MW Beam Power Operation of the J-PARC Main Ring”, *Prog. Theor. Exp. Phys.*, vol. 2021, p. 033G01, 2021. doi: 10.1093/ptep/ptab011

[15] Y. Hashimoto *et al.*, “Multi-ribbon Profile Monitor Using Carbon Graphite Foil for J-PARC”, in *Proc. HB'10*, Morschach, Switzerland, Sep.-Oct. 2010, paper WEO2A01, pp. 429-433.

[16] K. Sato, “Development of a Multi-Ribbon Profile Monitor in a beam dump line of J-PARC MR”, MA theses, UTokyo, Tokyo, Japan, 2020.

[17] K. Sakashita, Preliminary data, Private communication.

[18] M. Friend, “Challenges in continuous beam profile monitoring for MW-power proton beams”, in *Proc. IBIC'19*, Malmö, Sweden, Sep. 2019, pp. 253-256. doi: 10.18429/JACoW-IBIC2019-TUB003